JOURNAL OF BACTERIOLOGY, May 2009, p. 3086–3094 Vol. 191, No. 9
0021-9193/09/$08.00+0 doi:10.1128/JB.01037-08

Spatial Arrangement of the β-Glucoside Transporter from *Escherichia coli*▽†

Sharon Yagur-Kroll, Ayelet Ido, and Orna Amster-Choder*

Department of Molecular Biology The Hebrew University—Hadassah Medical School, P.O. Box 12272, Jerusalem 91120, Israel

Received 27 July 2008/Accepted 18 February 2009

The *Escherichia coli* BglF protein, a sugar permease of the phosphoenolpyruvate-dependent phosphotransferase system (PTS), catalyzes concomitant transport and phosphorylation of β-glucosides across the cytoplasmic membrane. Despite intensive studies of PTS permeases, the mechanism that couples sugar translocation to phosphorylation and the nature of the translocation apparatus are poorly understood. Like many PTS permeases, BglF consists of a transmembrane domain, which in addition to transmembrane helices (TMs) contains a big cytoplasmic loop and two hydrophilic domains, one containing a conserved cysteine that phosphorylates the incoming sugar. We previously reported that the big hydrophilic loop, which connects TM VI to TM VII, contains regions that alternate between facing-in and facing-out states and speculated that it is involved in creating the sugar translocation channel. In the current study we used [2-(trimethylammonium)ethyl]methanethiosulfonate bromide (MTSET), a membrane-impermeative thiol-specific reagent, to identify sites that are involved in sugar transport. These sites map to the regions that border the big loop. Using cross-linking reagents that penetrate the cell, we could demonstrate spatial proximity between positions at the center of the big loop and the phosphorylation site, suggesting that the two regions come together to execute sugar phosphotransfer. Additionally, positions on opposite ends of the big loop were found to be spatially close. Cys accessibility analyses suggested that the sugar induces a change in this region. Taken together, our results demonstrate that the big loop participates in creating the sugar pathway and explain the observed coupling between translocation of PTS sugars from the periplasm to the cytoplasm and their phosphorylation.

The phosphoenolpyruvate-dependent carbohydrate phosphotransferase system (PTS) is a central system in bacteria that controls preferential use of carbon sources. In addition to catabolite repression and inducer exclusion, the PTS is responsible for the translocation of a variety of energetically favorable carbohydrates across the cytoplasmic membrane and for their concomitant phosphorylation (10). It consists of two general PTS proteins, enzyme I and HPr, and a number of sugar-specific permeases. The phosphorylation cascade starts with enzyme I, which accepts a phosphoryl group from phosphoenolpyruvate and passes it on to HPr; the latter molecule phosphorylates the sugar-specific permeases. BglF (also designated EII^{bgl}) is a PTS permease that catalyzes phosphotransfer of β-glucosides into *Escherichia coli* cells (13). Like many other PTS permeases, BglF is composed of three conserved domains (for reviews, see references 27 and 22): the hydrophilic A and B domains and the membrane C domain (corresponding to the IIA^{bgl}, IIB^{bgl}, and IIC^{bgl} domains, respectively). The A domain is phosphorylated at H547 by HPr; the phosphate is then transferred to C24 in the B domain and subsequently to the incoming β-glucosides (8, 28). In addition, BglF regulates the transcriptional antiterminator BglG, depending on β-glucoside availability, by reversibly phosphorylating it via the same residue that phosphorylates the incoming sugar, C24 (2, 3, 4, 8, 9). The membrane domain of PTS permeases is assumed to form the sugar translocation channel. The nature of the channel and the mechanism that guarantees coupling between translocation of PTS sugars and phosphorylation are poorly understood (10, 20).

To try to elucidate the nature of the sugar translocation channel formed by the PTS permeases, their membrane domain was systematically investigated by using different strategies. These studies suggested that there are six to eight transmembrane helices (TMs) and that there is one large hydrophilic loop (consisting of more than 80 residues) at the cytoplasmic side of the membrane (22). Several residues in this loop, particularly the strongly conserved GIXE motif, appear to have an important role in sugar binding and/or phosphorylation (22). Based on Cys replacement mutagenesis and the accessibility of the cysteines to thiol-specific reagents in vivo, we recently proposed a two-dimensional model for the membrane topology of BglF (34). Based on our results, the membrane domain of BglF consists of eight TMs (TM I to TM VIII), and the region that connects TM VI and TM VII, the alleged big cytoplasmic loop that contains the GIXE motif, contains regions that are occasionally exposed to the periplasm. This finding and other findings suggested that this region is involved in sugar translocation and that its conformation is affected by the sugar (34).

To further investigate the elements involved in sugar uptake and the mechanism that couples sugar translocation and phosphorylation, we took several experimental approaches. By inhibiting sugar phosphotransfer with the impermeative thiol-specific reagent [2-(trimethylammonium)ethyl]methanethiosulfonate bromide (MTSET), we identified sites that are involved in transporting the sugar into the cell. All the residues affected by

* Corresponding author. Mailing address: Department of Molecular Biology The Hebrew University—Hadassah Medical School, P.O. Box 12272, Jerusalem 91120, Israel. Phone: 972 2 675 8460. Fax: 972 2 6747910. E-mail: amster@cc.huji.ac.il.

† Supplemental material for this article may be found at http://jb.asm.org/.

▽ Published ahead of print on 27 February 2009.

MTSET map to regions that border the big loop, thus strongly supporting our previous hypothesis that the big loop and its margins participate in creating the sugar translocation channel. The accessibility of these residues to the hydrophilic MTSET reagent suggests that the sugar pathway is an aqueous environment. Cross-linking studies demonstrated that C24, the phosphorylating residue, is located near the center of the big loop, in the vicinity of the GITE motif, and that the ends of the hydrophilic loop are spatially close. These results explain the observed coupling between transport of the incoming sugar and its phosphorylation and suggest that the hydrophilic loop forms a polar sugar pathway. Finally, the effect of the sugar on the accessibility of residues in the big loop to an impermeable thiol-specific reagent reinforced the idea that this region is occasionally exposed to the periplasm and suggested that the sugar induces a change in the translocation channel.

MATERIALS AND METHODS

Chemicals. 1,6-Bismaleimidohexane (BMH) and dithio-bismaleimidoethane (DTME) were obtained from Pierce. *N*,*N*-(*p*-Phenylene)dimaleimide (*p*-PDM), *N*,*N*-(*o*-phenylene)dimaleimide (*o*-PDM), *p*-nitrophenyl-β-D-glucopyranoside (*p*NPG), salicin, endonuclease (Benzonase), rifampin, *N*,*N*-dimethylformamide (DMF), isopropyl-1-thio-β-D-galactopyranoside (IPTG), lysozyme, DNase, RNase, DL-dithiothreitol (DTT), *N*-ethylmaleimide (NEM), and methionine were obtained from Sigma. The protease inhibitor 4-(2-aminoethyl)-benzenesulfonyl-fluoride hydrochloride was obtained from Calbiochem. Ni-nitrilotriacetic acid resin was obtained from Qiagen. Fluorescein-5-maleimide (5-FM) was obtained from Pierce. 2-Aminoethyl methanethiosulfonate hydrobromide (MTSEA) and MTSET were obtained from Toronto Research Chemical Inc. L-[^{35}S]methionine was obtained from Amersham Pharmacia Biotech.

Strains. The following *E. coli* K-12 strains were used. AG1688 [MC1061 (F′ 128 *lacI*^{q} *lac*::Tn*5*)] was used for construction of di- and tri-Cys BglF mutants; K38 (HfrC *trpR thi* λ^{+}), obtained from C. Richardson, was used for [^{35}S]methionine labeling of the different BglF variants; and HMS174(DE3) [F^{-} *recA1* *hsdR*(r_{K12}^{-} m_{K12}^{+}) Rif^{r} (DE3)], obtained from Novagen, was used for assaying sugar phosphotransfer, for examining accessibility to thiol-specific reagents, and for monitoring expression of the BglF variants as His-tagged proteins.

Plasmids. Plasmids encoding di-Cys BglF variants were constructed as described previously (34). In short, a BglF variant in which all the native cysteines except C24 were replaced by serines (C24-only variant) was used as a background to construct a set of plasmids that encoded BglF mutants that contain the active site cysteine and another cysteine in the C or A domain. Tri-Cys mutants were constructed by fragment exchange using restriction enzymes. The *bglF* alleles were cloned in pET15b to generate N′-terminal His-tagged BglF variants. pGP1-2, which carries the T7 RNA polymerase gene under control of the lambda *c*I857 repressor, was obtained from Life Technologies, Inc. All mutations were confirmed by sequencing.

Inhibition of β-glucoside phosphotransfer by MTSET. Phosphotransfer of the β-glucoside *p*NPG was assayed in HMS174(DE3) cells expressing the different BglF proteins as previously described (34), except that, where indicated, cells were incubated in the presence or absence of freshly prepared 1 mM MTSET for 5 min at 37°C prior to *p*NPG addition.

Metabolic labeling and in vivo cross-linking of proteins. The methods used for growth, induction, and [^{35}S]methionine labeling were essentially the methods described previously (2). In short, *E. coli* K38 cells containing derivatives of pT7OAC-F, which encode single- or di-Cys BglF proteins cloned under T7 promoter control, and pGP1-2, which encodes the heat-inducible T7 RNA polymerase gene, were grown in minimal medium with 0.4% succinate as the sole carbon source. At an optical density at 600 nm of 0.3, expression of the T7 RNA polymerase and hence expression of BglF were induced by shifting the culture either to 37°C or to 42°C. After 20 min, rifampin at a final concentration of 200 μg/ml was added to inhibit the activity of the *E. coli* RNA polymerase and hence prevent transcription of all genes except the plasmid *bglF* alleles that are transcribed by the T7 RNA polymerase. Cells were incubated further for 10 min at 37°C or 42°C and for 30 min at 30°C and then labeled with [^{35}S]methionine (14.3 mCi/ml) for 5 min. Unlabeled methionine was then added to a final concentration of 0.5 mg/ml to the growth medium, and the culture was incubated for another 5 min. Eight aliquots (0.5 ml) were pelleted by centrifugation, washed with phosphate-buffered saline (PBS) (pH 7) (20 mM sodium phosphate buffer and 150 mM NaCl, pH 7), pelleted again, and resuspended in 50 μl of PBS (pH 7.0). Salicin (final concentration, 0.2%) was added to four aliquots, PBS was added to the other four aliquots, and the cells were incubated at room temperature for 5 min. Subsequently, *o*-PDM, *p*-PDM, or BMH (final concentration, 1 mM) from a 50 mM stock solution in DMF or only DMF (final concentration, 2%) was added to the sugar-treated and untreated aliquots and incubated for 45 min at 30°C. The reaction was quenched by addition of NEM (final concentration, 10 mM) and DTT (final concentration, 10 mM) for 5 min at room temperature. Treatment of cells with DTME (final concentration, 1 mM) was performed similarly, except that cells were incubated with the cross-linker for 30 min at 30°C, washed once with PBS, and incubated either with DTT (final concentration, 100 mM) or with water for 5 min at room temperature. Electrophoresis sample buffer lacking reducing agents but containing 10 U of the endonuclease Benzonase was added, and the samples were incubated for 10 min at 30°C. BglF dimers were broken by incubation at 80°C for 5 min. Electrophoresis of proteins was carried out on 7.5% sodium dodecyl sulfate (SDS)-polyacrylamide gels. The protocol used for detecting disulfide bonds in vivo was the same, except that chemical cross-linkers were not added. When indicated, DTT (final concentration, 100 mM) was added to the samples for 5 min at room temperature before sample buffer was added, and the proteins were analyzed on 7.5% SDS-polyacrylamide gels. After electrophoresis, all gels were directly dried and exposed to Kodak BioMax MR film. The intensity of the bands was quantified using the TINA 2.0 software. The efficiency of cross-linking was calculated as described in Table S1 in the supplemental material.

Cysteine accessibility to the 5-FM reagent in whole cells. The methods used for growth and induction of HMS174(DE3) cells expressing di-Cys BglF variants were essentially the methods described previously (34). Cells expressing di-Cys BglF variants were incubated for 10 min at 25°C with or without freshly prepared salicin at a final concentration of 0.2%. Then 5-FM was added at a final concentration of 0.25 mM, and the culture was incubated for another 10 min. The cells were washed, and the labeled proteins were purified, denatured, and analyzed as described previously (34). The protein content in each lane was evaluated by staining the same gel with Coomassie brilliant blue. The amounts in the fluorescent BglF bands were normalized to the amounts in the stained bands using the TINA 2.0 software.

RESULTS

Regions on both sides of the big hydrophilic loop in the membrane domain are involved in sugar phosphotransfer. To identify sites in BglF that are important for sugar phosphotransfer, we studied the effect of MTSET, a membrane-impermeable thiol-specific reagent, on β-glucoside phosphotransfer in vivo using a collection of 30 di-Cys BglF variants. All these variants contained C24 and either one of the other seven native cysteines of BglF or a cysteine introduced at various positions in the C24-only variant (a BglF derivative that lacks the seven other endogenous cysteines). These variants were shown to catalyze the various activities of BglF; their levels of expression were shown to guarantee correct insertion of BglF proteins in the membrane; and their abilities to catalyze sugar phosphotransfer of three β-glucosides arbutin, salicin, and *p*NPG were shown to be comparable (34). Here, the ability of all these di-Cys mutants to consume the β-glucoside *p*NPG after MTSET addition was assayed. Hydrolysis of P~*p*NPG, which directly correlates with sugar phosphotransfer, generates a yellow color, whose intensity can be quantified by measuring the absorbance at 410 nm (see Materials and Methods). Figure 1 shows the level of activity of each variant in the presence of MTSET relative to the activity of the same variant without MTSET. Cells not expressing BglF or expressing either a Cys-less BglF derivative or a BglF mutant that lacks the phosphorylation site (C24S) were inactive in *p*NPG hydrolysis independent of MTSET addition, indicating that *p*NPG is transported into the cell only by BglF. As shown in Fig. 1, the

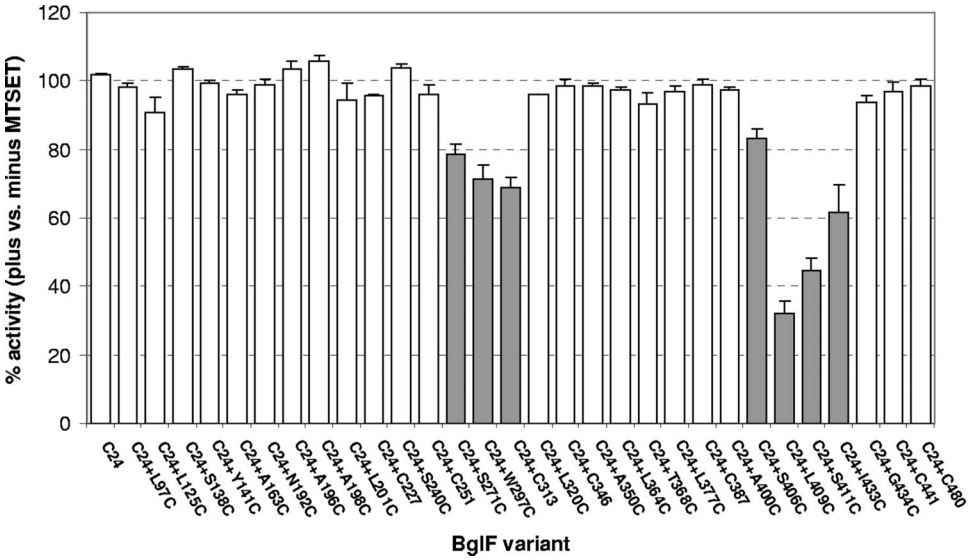

FIG. 1. Effect of MTSET on β-glucoside phosphotransfer. Cells expressing the different BglF variants were incubated with or without MTSET. The β-glucoside *p*NPG was added for 10 min, and the ability of the BglF proteins to utilize this sugar was assayed as described in Materials and Methods. The data are the sugar phosphotransfer activity of each variant after exposure to MTSET relative to the activity of the same variant that was not exposed to MTSET expressed as a percentage. Cells not expressing BglF or expressing a Cys-less BglF derivative or the C24S BglF mutant were inactive for *p*NPG hydrolysis, independent of MTSET addition. Open bars, mutants not affected by MTSET (less than 10% inhibition); filled bars, mutants inhibited by MTSET. The results are the averages of at least three independent experiments. The standard deviations for the different experiments are indicated by the error bars.

activity of the C24-only variant, which is the parental strain of all of the BglF di-Cys mutants, was not inhibited by the addition of the impermeable MTSET reagent. Hence, by analyzing the phosphotransfer activity of the di-Cys mutants, all containing the C24 active site and an additional cysteine, we could examine which Cys replacement is affected in response to MTSET addition. The activity of most di-Cys variants was not inhibited by the addition of MTSET prior to sugar addition (less than 10% inhibition), indicating that the mutant positions are located in regions that are not essential for sugar translocation or are not available for the impermeable MTSET reagent (Fig. 1). The activities of seven mutants were inhibited by MTSET to various degrees (Fig. 1). The most dramatic inhibition was observed with a mutant that has a cysteine at position 409, whose activity in the presence of MTSET was 32% of its activity without MTSET (i.e., 68% inhibition). The activity of a mutant with a cysteine at a nearby position, position 411, was also significantly inhibited (55% inhibition). The levels of inhibition of the other five mutants by MTSET ranged from 18 to 39%. Four of the seven variants, the variants with Cys replacement at either position 297, 313, 409, or 433, showed lower activity than the C24-only variant even before MTSET addition, but the other three mutants exhibited activity that was comparable to that of the C24-only variant (34). Noticeably, the seven cysteines whose interaction with MTSET interfered with the sugar phosphotransfer process are clustered in two regions, the termini of the alleged big cytoplasmic loop. These regions have previously been shown to alternate between the cytoplasm and the periplasm (34).

We repeated the experiments described above with MTSES [sodium (2-sulfonatoethyl)methanethiosulfonate], a thiol-specific impermeable reagent that is similar to MTSET but is negatively charged, whereas MTSET is positively charged. A pattern of inhibition similar to the pattern described above was observed when the di-Cys BglF variants were treated with MTSES, but the levels of inhibition were slightly lower (data not shown). Taken together, our results demonstrate that the binding of thiol-specific reagents to positions located at both edges of the big hydrophilic loop inhibits sugar phosphotransfer activity, supporting the theory that this region forms the sugar translocation channel. It is notable that position 409, which exhibits the highest sensitivity to the thiol-specific reagents, was shown by us previously to be accessible from the periplasm to both thiol reagents and β-glucosides (34). Moreover, not only does MTSET prevent access of the sugar to this position, as demonstrated here, but the sugar was shown to prevent access of MTSET to this position (34).

BglF phosphorylation site is spatially close to the big hydrophilic loop in the membrane domain. Catalysis of sugar transport by PTS permeases, such as BglF, is coupled to sugar phosphorylation. To understand the structural basis for this coupling, we aimed to study the spatial arrangement of the phosphorylation site or domain, relative to the other domains of BglF, mainly the sugar-transporting domain. To identify positions that are spatially close to the C24 phosphorylation site, we tested the possibility of chemically cross-linking C24 in vivo to the second cysteine in our collection of di-Cys BglF variants. To this end, cells expressing the di-Cys variants were metabolically labeled with [^{35}S]methionine under conditions in which the BglF proteins are specifically labeled (2) (see Fig. S1, lanes 1, in the supplemental material), and then the cells were incubated with cell-penetrating thiol-specific cross-linking reagents. The low level of expression of the BglF proteins in this experimental system necessitated radioactive labeling to enable detection of the proteins. As cross-linkers we used three homo-bifunctional reagents, BMH, *p*-PDM, and *o*-PDM.

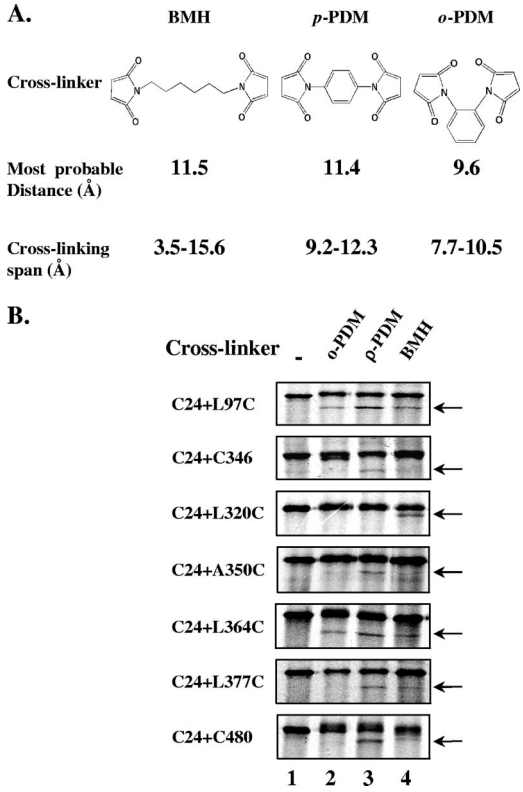

FIG. 2. In vivo chemical cross-linking between C24 and the second cysteine of di-Cys BglF proteins. (A) The three homo-bifunctional cysteine cross-linkers used. (B) Di-Cys BglF derivatives were specifically labeled with [^{35}S]methionine as described in Materials and Methods. Cells were pelleted, washed, resuspended with PBS, and incubated with BMH, *p*-PDM, or *o*-PDM dissolved in DMF or with only DMF. The reaction was quenched by addition of NEM and DTT, as described in Materials and Methods. Proteins were denatured in electrophoresis sample buffer and analyzed on 7.5% SDS-polyacrylamide gels, followed by autoradiography. Results are presented only for BglF variants that generated cross-links. The arrows indicate the positions of the cross-linked products of BglF.

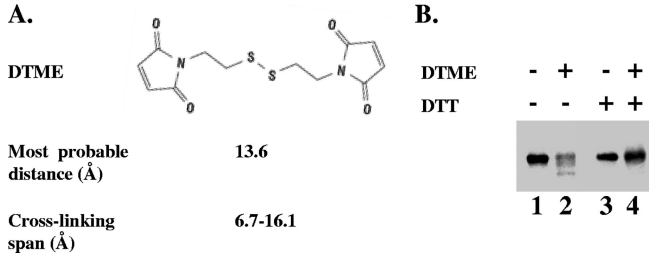

FIG. 3. Generation of reversible cross-links between C24 and a second cysteine in a di-Cys BglF protein in vivo. (A) DTME, a sulfhydryl-reactive homo-bifunctional cross-linker, contains an internal disulfide that can be cleaved by reducing agents. (B) The C24-C480 di-Cys BglF variant was specifically labeled with [^{35}S]methionine. Cells were incubated with or without the cleavable cross-linker DTME, washed with PBS, and incubated either with DTT or with water (see Materials and Methods). Proteins were analyzed by SDS-polyacrylamide gel electrophoresis as described in the legend to Fig. 2.

These reagents have two maleimides connected by a flexible (BMH) or rigid (*p*-PDM and *o*-PDM) linker, and their ranges of cross-linking partially overlap (16) (Fig. 2A).

As shown in Fig. 2B, 7 of the 33 di-Cys mutants that were tested produced an additional faster-migrating labeled band on an SDS-polyacrylamide gel after incubation with one or more cross-linkers compared to the results for the nontreated proteins (the entire gels, showing the results for representative mutants that did or did not generate cross-links, are shown in Fig S1 in the supplemental material). The faster-migrating bands were not observed after incubation of a parallel set of single-Cys variants with the cross-linkers, although the individual cysteines reacted with the cross-linkers, as shown by the slight retardation of the migration of the entire protein portion or a fraction of it on an SDS-polyacrylamide gel (see Fig. S2 in the supplemental material). Confirmation that intramolecular cross-linked BglF proteins migrate faster on SDS-polyacrylamide gels was obtained by using a cleavable cross-linker. DTME is a sulfhydryl-reactive homo-bifunctional cross-linker which has a cross-linking range partially overlapping those of the other reagents that we used (16) and which contains an internal disulfide that can be cleaved by reducing agents (Fig. 3A). The faster-migrating band detected after treatment of cells expressing di-Cys BglF mutants with DTME exhibited the original electrophoretic migration after the addition of DTT (Fig. 3B). Apparently, the intramolecular cross-linked BglF proteins migrate faster because they cannot be fully spread when they are denatured.

The in vivo cross-linking results obtained with all 33 di-Cys mutants in several independent experiments are summarized in Table S1 in the supplemental material. The results were highly reproducible, and there was no ambiguity about the existence and pattern of cross-linking in all cases. Comparable results were obtained when the cultures expressing the BglF proteins were shifted to 37°C or to 42°C (to induce the heat-inducible T7 RNA polymerase gene [see Materials and Methods]), ruling out the possibility that formation of cross-linked products is related to heat (data not shown). Our results demonstrate that, by and large, C24 cross-linked with cysteines in the alleged big cytoplasmic loop, including the cysteine at position 364 that is adjacent to the conserved GIXE motif, although not with all cysteines in this region. Two exceptions that also cross-linked with C24 were C480, located in the A domain that phosphorylates C24, and the cysteine at position 97, located in the linker that connects the B and C domains.

Several of the seven di-Cys mutants that generated cross-links exhibited cross-linking with more than one reagent (Fig. 2B). This can be explained by the overlap in the range of the S-S distances that can be bridged by these reagents. Alternatively, it can be explained by the slight movement of the domains, leading to minor changes in the distance between the two cysteines. The fact that the highest-efficiency cross-linking was observed with a rigid cross-linker, *p*-PDM, rather than with the flexible reagent BMH, which covers the entire span width of *p*-PDM, suggests that the results are a reflection of genuine proximity rather than domain movement that enables occasional interactions.

The other 26 cysteines in the membrane domain showed no cross-linking with C24 (see Table S1 in the supplemental material), suggesting that they are not close enough to C24. It is unlikely that this is due to inaccessibility of these cysteines to

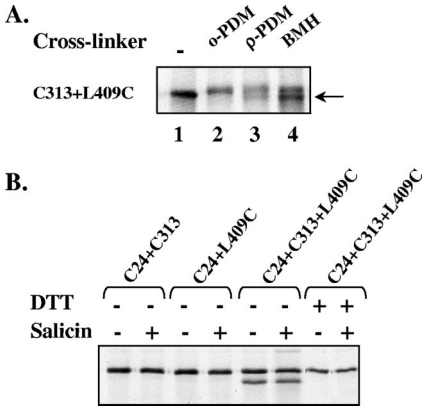

FIG. 4. In vivo spatial proximity of positions located on opposite sides of the alleged big loop. (A) Cells expressing a BglF derivative containing C24 and two additional cysteines at positions 313 and 409 were labeled with [^{35}S]methionine and treated with cross-linking reagents, and their proteins were analyzed as described in the legend to Fig. 2B. Proteins were denatured in electrophoresis sample buffer and analyzed on 7.5% SDS-polyacrylamide gels, followed by autoradiography. (B) Cells expressing di- and tri-Cys BglF derivatives, as indicated above the lanes, were grown and metabolically labeled as described above for panel A, except that cross-linkers were not added. Where indicated, 0.2% salicin was added to the cells for 5 min. DTT was added to the cells only where indicated. Proteins were analyzed on 7.5% SDS-polyacrylamide gels and detected by autoradiography.

the cross-linkers, because all of them except the few buried in the membrane were shown to react with thiol-specific reagents (34). The finding that C24 did not cross-link with any of the cysteines predicted to face the periplasm or to be buried in the membrane substantiates not only the reliability of the cross-linking results but also the topological model that we previously proposed (34). The results indicate that C24 is spatially close to the cytoplasmic face of the membrane domain, particularly to positions in the alleged cytoplasmic loop, a presumed constituent of the translocation channel.

Spatial proximity between the ends of the big hydrophilic loop. To investigate the spatial arrangement of the putative sugar channel, we examined the possibility that positions on opposite sides of the big hydrophilic loop, which is part of the membrane domain, are spatially close. To address this question, we asked whether a cysteine at position 409, located near the C′ terminus of the big loop, can be cross-linked in vivo to cysteines located at the other end of the loop, whose activity was inhibited by MTSET. Since it was crucial that all of the variants tested were active, all mutants had to contain the active site C24. Therefore, we constructed several BglF variants that contain three cysteine residues: the active site C24, a cysteine at position 409, and a third cysteine at the other end of the big loop. The positions that we chose, including position 409, did not produce a cross-link with the C24 active site (based on the results described above). Therefore, if cross-linking was observed with the triple mutants, it was evidence of the proximity of position 409 and the third cysteine residue. Cells expressing the tri-Cys variant were metabolically labeled with [^{35}S]methionine, and cross-linking was carried out in vivo using the reagents used in the experiments described above. Figure 4A shows that positions 409 and 313 could be cross-linked, suggesting that positions located at opposite ends of the big loop are in close proximity.

To learn more about the distance between the opposite ends of the big hydrophilic loop that seems to form the core of the sugar channel, we tested whether cysteines 409 and 313 can come close enough to form a disulfide bond, defined as zero-length cross-linking. To this end, we analyzed the tri-Cys variant containing cysteines at positions 24, 313, and 409 and the di-Cys mutants containing C24 and C313 and containing C24 and S409C by SDS-polyacrylamide gel electrophoresis in the absence of reducing agents with and without the stimulating sugar. As shown in Fig. 4B, only the tri-Cys mutant was able to form a disulfide bond, which disappeared in the presence of DTT. The disulfide bond was also detected after the addition of salicin, albeit at a somewhat lower frequency. These results indicate that positions 313 and 409 can be in very close proximity, as the length of a disulfide bond is ~2 Å. The fact that these two positions can be found at a distance that is either as short as 2 Å (S-S bond) or as long as 12 Å or more (crossed by BMH) suggests that there is a high degree of flexibility in the distance between these residues and within the sugar translocation channel. It is important to note that the formation of the disulfide bond was spontaneous; that is, there was no catalyst to initiate oxidation. It is also important to mention that NEM, which interacts with free thiols, was added before cells ruptured. Thus, the S-S bond between positions 313 and 409 is formed in vivo in a considerable portion of the cell population and is not a product of oxidation after cells lysis.

Positions in the big hydrophilic loop are accessible to the membrane-impermeable reagent 5-FM. To further explore the role of residues in the suggested sugar translocation channel in BglF conformation and function, the accessibility of cysteines in this region to 5-FM and the effect of the β-glucoside salicin on this accessibility were tested. 5-FM is a thiol-specific fluorescent reagent that is known to be impermeable and to react with sulfhydryl groups in polar environments but not in apolar environments (25, 26, 35). To perform this experiment, whole cells expressing di-Cys BglF derivatives containing the internal active site C24 and having cysteine substitutions in the big loop were incubated with 5-FM after incubation of the cells with or without salicin. The cells were subsequently washed and lysed, the membranes were pelleted, and the His-tagged BglF mutants were denatured and affinity purified. Labeling was monitored by using the fluorescence of BglF bands on SDS-polyacrylamide gels. The degrees of fluorescent labeling were normalized to the amounts of protein in the corresponding bands in the Coomassie blue-stained gel. As shown in Fig. 5, the C24-only variant, which was the background for all other di-Cys variants that were tested, was not accessible to 5-FM regardless of the stimulating sugar. For this reason, we could test the other di-Cys variants, all containing the active site C24, and learn about the accessibility of the second cysteine in these mutants. Position 377, located in the middle of the loop, became accessible to 5-FM only upon sugar addition (Fig. 5). The other di-Cys variants shown in Fig. 5, all having a cysteine near an end of the big loop, exhibited the opposite pattern; i.e., they were accessible to 5-FM in the absence of the stimulating sugar, while the accessibility of the positions to 5-FM decreased in the presence of the inducer. All other Cys replacements in this loop (i.e., replacements at positions 297, 313, 346,

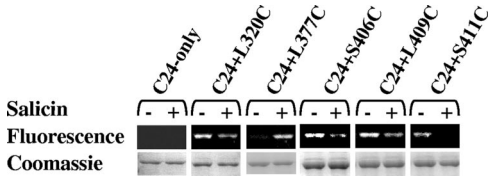

FIG. 5. Effect of β-glucoside on cysteine accessibility to 5-FM. Whole cells expressing the C24-only variant or di-Cys variants were incubated for 10 min at 25°C with or without 0.2% salicin. 5-FM (0.25 mM) was added for another 10 min. The cells were washed, and the proteins were purified using Ni-chelate chromatography. The proteins were analyzed on 10% SDS-polyacrylamide gels, and the fluorescence profile was compared to the protein content after Coomassie blue staining.

350, 364, 368, 387 and 400) showed no accessibility to 5-FM regardless of the presence of the stimulating sugar (data not shown). It is likely that the effect of the sugar on some residues directly prevents access of 5-FM. However, this could not explain the sugar-induced increase in the accessibility of position 377 to 5-FM. Hence, a likely explanation, which is not mutually exclusive with the previous explanation, is that the effect of the sugar was indirect due to induction of a conformational change in the channel so that residues that were accessible became inaccessible and vice versa. In addition, the fact that residues in this region are reactive with the impermeable 5-FM reagent strongly supports our suggestion that this loop is not simply cytoplasmic and that residues within the loop occasionally face the periplasm.

DISCUSSION

Sugar permeases of PTS have been intensively studied for many years, yet the elements that recognize the sugar, the nature of the translocation channel, and the mechanism that couples sugar translocation through the membrane to sugar phosphorylation by a hydrophilic domain are largely unknown. In the current work, we took several approaches to advance our understanding of sugar phosphotransfer by PTS permeases. The first step was to identify sites in the membrane domain of the β-glucoside phosphotransferase, BglF, that are important for sugar uptake. We examined the ability of Cys replacement mutants to perform sugar phosphotransfer in the presence of MTSET, a small, flexible, and positively charged reagent that reacts rapidly and specifically with the sulfhydryl groups of cysteines under physiological conditions (1). This method has been used to determine pore-lining residues in numerous membrane proteins, including the lactose permease of *E. coli* (11), the mouse acetylcholine receptor (1), the human glucose transporter Glut1, and the human anion exchanger isoform 1 (31). Because the active site of BglF is a cysteine residue, we could not use any thiol reagent that would react with it and would inactivate the protein. For example, MTSEA, a thiol-specific reagent that penetrates the cell, inactivated the internal C24 active site (data not shown). We therefore chose MTSET, which does not penetrate the cell (1), and used it under the conditions previously shown by us not to inactivate C24 (34).

The model shown in Fig. 6A incorporates many of the results presented in this study into the predicted membrane topology of a BglF monomer that we have suggested previously (34). All the positions whose binding to MTSET affected sugar phosphotransfer (Fig. 6A) lie near the ends of the big loop that connect TM VI and TM VII or in the two periplasmic loops found on either side of the big loop. These three loops and the two TMs connecting them were previously suggested by us to form a module with inherent dynamics, as it contains residues that are occasionally accessible from either the periplasmic or cytoplasmic side (34). We predicted that this module creates the sugar translocation channel or constitutes an important part of it. The current results strongly support our theory and suggest that the two regions, to which the positions whose binding to MTSET inhibited BglF activity map, are part of the sugar pathway. Evidently, the specific residues that were blocked by MTSET are not essential for sugar transport, since they could be replaced by cysteines without abolishing activity (some replacements reduced the activity to some extent [34], but none of the replacements used here led to complete loss of activity). Rather, the regions surrounding these residues can be defined as regions important for sugar transport, since chemical modification in these regions impaired access of the sugar to the channel. Because MTSET is a billion times more reactive in aqueous solution than in a lipid environment (1, 23), the results also indicate that this pathway is a polar environment. Importantly, other external residues of BglF that were previously shown by us to react with MTSET under the experimental conditions employed here (i.e., L125 and L201 [34]) were not inhibited by this reagent. The fact that these residues showed no inhibition of sugar phosphotransfer activity by MTSET, even though they interact with it, validates our assay and makes the results more significant. It is reasonable to assume that if we could use a permeable thiol reagent, such as MTSEA or NEM, we could identify additional residues essential for the sugar translocation process.

Next, we attempted to obtain information on the spatial arrangement of the phosphorylating and translocating domains and sites of BglF. Because hydrophobic membrane proteins are notoriously difficult to crystallize, we aimed at obtaining structural information about BglF by chemical cross-linking. This approach is widely used for studying helix proximity, helix tilting, the proximity of periplasmic and cytoplasmic loops, dimer surface interactions, and ligand-induced distance changes (12, 18, 33). It is based on the assumption that cysteine cross-links are a measure of proximity. Indeed two cysteines can be cross-linked if they are highly chemically reactive or frequently undergo collisions. However, there is a strong correlation between collision rates and proximity (29). Comparison of proximities between periplasmic loops in the lactose permease that were estimated by spin labeling or by thiol cross-linking led to the conclusion that thiol cross-linking is primarily a reflection of proximity, whereas other factors, such as dynamics and reactivity, are of secondary importance (30). Lessons from lactose permease structural studies indicate that cross-linking is useful for detecting local interactions (17). Here we used it to study in vivo the imminence of the active site cysteine, C24, located in the hydrophilic B domain, to different positions in BglF, mainly in the membrane C domain, and the proximity between sequences at both ends of the big loop in the membrane domain.

Relatively low efficiencies of cross-linking are not uncom-

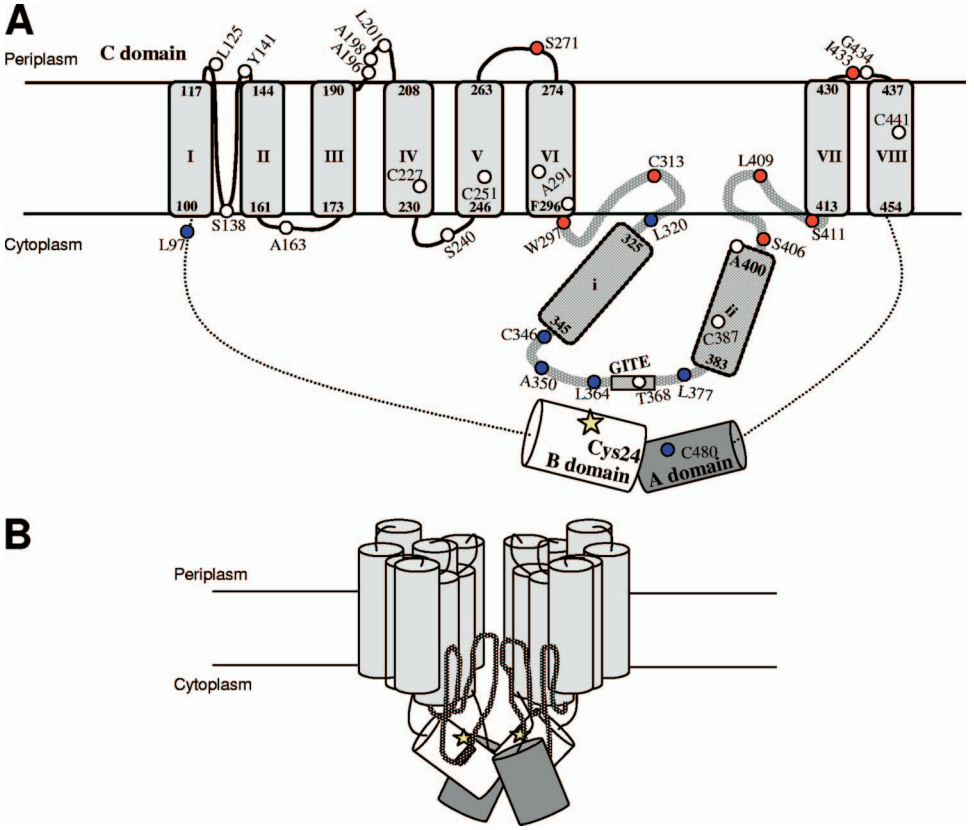

FIG. 6. (A) Predicted membrane topology of a BglF monomer. The model is adapted from the model of Yagur-Kroll and Amster-Choder (34). The topology for the vicinity between regions and domains is based on in vivo cross-linking data. The regions that participate in creating the sugar translocation channel were deduced from inhibition of sugar phosphotransfer by MTSET. The A and B domains are represented by a dark gray cylinder and an open cylinder, respectively. TMs in the C domain are represented by light gray cylinders that are labeled I to VIII. The predicted positions at the termini of each helix are indicated. The big cytoplasmic loop is represented by a thick patterned line, and the two putative α helices within it are labeled i and ii. The GITE motif is represented by a box. The C24 active site is indicated by a yellow star. Native cysteines and residues which were replaced by cysteines are represented by circles, and their positions are indicated. Positions that could be chemically cross-linked with C24 in vivo are indicated by blue circles. Positions whose binding to MTSET inhibited sugar phosphotransfer are indicated by red circles. (B) Model for BglF dimer. The model is based on data from the present study and previous studies (see text). The colors indicate the same things that they indicate in panel A. The A and B domains, which are represented by dark gray and open cylinders, respectively, were positioned in a way that enables the A domain of one monomer to phosphorylate the B domain of either the same monomer or the other monomer. The model does not make specific predictions concerning which helices hold the monomers together by hydrophobic interactions.

mon. In fact, it is accepted that the extent of cross-linking by dimaleimides represents underestimation of the genuine proportion of the molecules with proximal cysteines. This is due to competitive reactions that reduce the cross-linking efficiency (32), among which are binding of each cysteine to a different dimaleimide molecule, inactivation of one of the maleimide moieties of a dimaleimide by hydrolysis, and terminal oxidation of thiols to sulfonates (6). For the experiments reported here, the actual fraction of molecules with cysteines proximal to C24 is undoubtedly higher than the fraction observed for two additional reasons. First and foremost, our experiments were performed in vivo using whole cells, whereas most cross-linking studies described previously were carried out with membrane suspensions to increase uptake of the cross-linking reagents (12, 33). We chose to use whole cells despite the anticipated reduction in cross-linking efficiency to ensure that all the observed cross-links were cross-links to cysteines that are free in vivo. Second, C24 is phosphorylated in a fraction of the BglF proteins and hence is not available for cross-linking. Nevertheless, the high reproducibility of the results implies that the fraction of molecules that are not phosphorylated at C24 under certain growth conditions does not vary much. Hence, the spatial setting of this residue can be explored using this methodology. The use of several cross-linkers reinforces the conclusions regarding spatial proximity. Also, use of several reagents is recommended because cysteines at certain positions may be sterically favored to undergo cross-linking with a reagent that is a particular length or a reagent that can adopt a range of conformations due to rotations of the bonds that form the linker arm (16). Still, the low efficiencies of cross-linking prevented us from using this experimental approach to document the effect of β-glucosides on BglF arrangement. We were reluctant to draw conclusions based on the difference between two small numbers (i.e., the fractions that were cross-linked in the presence and in the absence of the sugar for each mutant). Therefore, we took another approach to study the effect of the sugar on BglF spatial arrangement, accessibility to 5-FM (see below).

In the current study, we focused on the arrangement of the monomer (i.e., intramolecular proximities). However, BglF and other PTS permeases were shown to dimerize, with contacts between the monomers provided by the membrane domain (7, 10). Figure 6B shows a model for the BglF dimer that combines information from the present study with data obtained in previous studies. The ability of the A domain of one monomer to phosphorylate the B domain of the other monomer (7) suggests that, at least in a fraction of the dimers, the monomers are not parallel and perhaps are even asymmetrical. Therefore, the A domain is depicted in our model (Fig. 6B) as a domain capable of phosphorylating the B domain of its own monomer (intramolecular) or that of the neighboring monomer (intermolecular). The method employed here for BglF detection (specific labeling of de novo-synthesized BglF) is not suitable for studying dimer arrangement. Although bands whose sizes could correspond to those of BglF dimers were detected with some of the di-Cys mutants in the presence of cross-linkers (mostly BMH [see Fig. S1 in the supplemental material]), we could not determine whether they correspond to homodimers of BglF or to heterodimers between BglF and auxiliary proteins. In the future, the experimental strategy can be modified to study dimer organization (i.e., intermolecular proximities). This can be achieved by mixing two solubilized membrane preparations, each containing a mutant with a different Cys replacement, in the presence of a cross-linker (32). Because the number of combinations of Cys replacements is fairly high, priority should be given to Cys replacements at the ends of transmembrane segments. The rationale behind this preference is that hydrophobic interactions were suggested to be involved in the dimerization of BglF and other PTS permeases, but cysteines at the hydrophobic core are not susceptible to cross-linking. A 5-Å projection map of the transmembrane domain of the mannitol permease, which suggested that the PTS permeases are oligomers of dimers (20), complicates the interpretation of such a study on the one hand but may provide important information on helix packing on the other hand.

A main conclusion from the cross-linking assays is that C24 is in close proximity to the cytoplasmic side of the membrane domain, particularly to certain residues in the big loop (Fig. 6A). Significantly, most residues facing the cytoplasm could not be cross-linked with C24. Moreover, only 5 of 13 residues tested in the big loop cross-linked to the active site. Within this region, cross-linking was observed mainly with cysteines located at the center of the loop, which is predicted to be in the cytoplasm, and with only one cysteine in a region that alternates between the face-in and face-out states. Except for the latter cysteine, the cysteines that cross-link with C24 are located in a 47-residue conserved motif of the glucose superfamily of PTS permeases, to which BglF belongs (24). The consensus motif for the entire superfamily includes, besides the GITE sequence, several other well-conserved residues, including L364, which was shown here to cross-link with C24. Hence, the interactions of C24 with residues in this region are not random, suggesting that there are structural constraints that limit the degree of flexibility of these proximal and colliding domains. The proximity of C24 to positions in the vicinity of the strongly conserved GIXE motif is consistent with the suggestion that this motif is involved in transferring the phosphoryl groups from the PTS permeases to their cognate carbohydrates (22). The cellular localization of this motif was considered somewhat enigmatic, as topological studies of certain PTS permeases placed this motif in the cytoplasm (22), but a location near the periplasm was also suggested (5). In light of our previous (34) and current results, a likely scenario is that, at least in BglF, this motif is located on the inner side of the translocation apparatus and ushers C24 to the incoming sugar. Hence, the phosphorylating cysteine and the translocation apparatus seem to be arranged in a way which facilitates transfer of the phosphoryl group to the incoming sugar. The proximity between C24 and residues on the inner side of the membrane domain was demonstrated only intramolecularly (i.e., within the BglF monomer). This result was incorporated into the models shown in Fig. 6A and 6B. Nevertheless, the possibility of intermolecular proximity between these regions cannot be ruled out.

To learn more about the spatial arrangement of the sugar translocation channel, we used the in vivo cross-linking approach to study the proximity between residues located on the alleged interior side of the channel. We could show that the N′ and C′ termini of the big loop are in close proximity, as position 409, located on one side, creates cross-links and even forms a disulfide bond with position 313, located on the other side of the same loop. The disulfide bond between these positions is formed in less than 30% of the molecules and to a somewhat lesser extent in the presence of sugar, leaving the rest of the molecules available for other interactions (e.g., interactions with MTSET and β-glucosides). The fact that these two positions could be cross-linked with all three cross-linkers tested and also form a disulfide bond indicates that this region is very flexible, as expected for a region that forms the channel through which the sugar is transferred. One possibility is that the two termini of the loop come together to serve as a gate for the sugar channel.

Finally, positions located in the big loop were shown to be accessible to 5-FM, demonstrating once again that residues in this region are occasionally accessible from the periplasmic side to the nonpenetrating reagent. Changes in the accessibility of these residues to 5-FM upon sugar addition were also demonstrated. These changes cannot be explained simply by sugar sequestration of the 5-FM reacting sulfhydryl groups, because at least one position became more accessible to 5-FM in the presence of sugar. A likely explanation is that the dynamic loop undergoes a conformational change upon sugar addition and positions at the ends of the channel lose their reactivity with 5-FM, while positions in the middle of the channel become reactive. These results reinforce the idea that the sugar translocation channel is a dynamic structure that undergoes conformational changes that are dependent on the presence of the stimulating sugar.

An "alternating access and release" mechanism has been suggested for transporter proteins whose structure has been solved, such as ABC and secondary active membrane transporters (19, 21). In this mechanism the transporter is believed to have two major alternating conformations, inward facing and outward facing. Interconversion of the two conformations, which relies on inherent dynamics of the protein, facilitates substrate translocation across the membrane. Structural and dynamic information at high resolution is required to determine

whether PTS permeases translocate their sugar substrates via a similar mechanism. One aspect that the mechanism should explain is that PTS sugar permeases have periplasmic and cytoplasmic substrate-binding sites with different affinities for the sugar (14, 15), whereas the transporters mentioned above use a single binding site that alternates between the compartments.

ACKNOWLEDGMENTS

This work was supported by the Israel Science Foundation founded by the Israel Academy of Sciences and Humanities.

We appreciate helpful discussions with Liat Fux and Galya Monderer-Rothkoff. We acknowledge Eitan Bibi, Baruch Kanner, Shimon Schuldiner, and Etana Padan for technical advice.

REFERENCES

1. **Akabas, M. H., D. A. Stauffer, M. Xu, and A. Karlin.** 1992. Acetylcholine receptor channel structure probed in cysteine-substitution mutants. Science **258:**307–310.
2. **Amster-Choder, O., F. Houman, and A. Wright.** 1989. Protein phosphorylation regulates transcription of the β-glucoside utilization operon in E. coli. Cell **58:**847–855.
3. **Amster-Choder, O., and A. Wright.** 1992. Modulation of dimerization of a transcriptional antiterminator protein by phosphorylation. Science **257:**1395–1398.
4. **Amster-Choder, O., and A. Wright.** 1990. Regulation of activity of a transcriptional antiterminator in E. coli. by phosphorylation. Science **249:**540–542.
5. **Buhr, A., and B. Erni.** 1993. Membrane topology of the glucose transporter of Escherichia coli. J. Biol. Chem. **268:**11599–11603.
6. **Careaga, C. L., and J. J. Falke.** 1992. Thermal motions of surface alpha-helices in the D-galactose chemosensory receptor. Detection by disulfide trapping. J. Mol. Biol. **226:**1219–1235.
7. **Chen, Q., and O. Amster-Choder.** 1998. BglF, the sensor of the bgl system and the beta-glucosides permease of Escherichia coli: evidence for dimerization and intersubunit phosphotransfer. Biochemistry **37:**8714–8723.
8. **Chen, Q., J. C. Arents, R. Bader, P. Postma, and O. Amster-Choder.** 1997. BglF, the sensor of the *E. coli bgl* system, uses the same site to phosphorylate both a sugar and a regulatory protein. EMBO J. **16:**4617–4627.
9. **Chen, Q., P. W. Postma, and O. Amster-Choder.** 2000. Dephosphorylation of the *Escherichia coli* transcriptional antiterminator BglG by the sugar sensor BglF is the reversal of its phosphorylation. J. Bacteriol. **182:**2033–2036.
10. **Deutscher, J., C. Francke, and P. W. Postma.** 2006. How phosphotransferase system-related protein phosphorylation regulates carbohydrate metabolism in bacteria. Microbiol. Mol. Biol. Rev. **70:**939–1031.
11. **Dunten, R. L., M. Sahin-Toth, and H. R. Kaback.** 1993. Cysteine scanning mutagenesis of putative helix XI in the lactose permease of Escherichia coli. Biochemistry **32:**12644–12650.
12. **Ermolova, N., L. Guan, and H. R. Kaback.** 2003. Intermolecular thiol cross-linking via loops in the lactose permease of Escherichia coli. Proc. Natl. Acad. Sci. USA **100:**10187–10192.
13. **Fox, C. F., and G. Wilson.** 1968. The role of a phosphoenolpyruvate-dependent kinase system in β-glucoside catabolism in E. coli. Proc. Natl. Acad. Sci. USA **59:**988–995.
14. **Garcia-Alles, L. F., V. Navdaeva, S. Haenni, and B. Erni.** 2002. The glucose-specific carrier of the Escherichia coli phosphotransferase system. Eur. J. Biochem. **269:**4969–4980.
15. **Garcia-Alles, L. F., A. Zahn, and B. Erni.** 2002. Sugar recognition by the glucose and mannose permeases of Escherichia coli. Steady-state kinetics and inhibition studies. Biochemistry **41:**10077–10086.
16. **Green, N. S., E. Reisler, and K. N. Houk.** 2001. Quantitative evaluation of the lengths of homobifunctional protein cross-linking reagents used as molecular rulers. Protein Sci. **10:**1293–1304.
17. **Guan, L., and H. R. Kaback.** 2006. Lessons from lactose permease. Annu. Rev. Biophys. Biomol. Struct. **35:**67–91.
18. **Guan, L., A. B. Weinglass, and H. R. Kaback.** 2001. Helix packing in the lactose permease of Escherichia coli: localization of helix VI. J. Mol. Biol. **312:**69–77.
19. **Hollenstein, K., R. J. Dawson, and K. P. Locher.** 2007. Structure and mechanism of ABC transporter proteins. Curr. Opin. Struct. Biol. **17:**412–418.
20. **Koning, R. I., W. Keegstra, G. T. Oostergetel, G. Schuurman-Wolters, G. T. Robillard, and A. Brisson.** 1999. The 5 A projection structure of the transmembrane domain of the mannitol transporter enzyme II. J. Mol. Biol. **287:**845–851.
21. **Lemieux, M. J., Y. Huang, and D. N. Wang.** 2004. The structural basis of substrate translocation by the Escherichia coli glycerol-3-phosphate transporter: a member of the major facilitator superfamily. Curr. Opin. Struct. Biol. **14:**405–412.
22. **Lengeler, J. W., K. Jahreis, and U. F. Wehmeier.** 1994. Enzymes II of the phospho enol pyruvate-dependent phosphotransferase systems: their structure and function in carbohydrate transport. Biochim. Biophys. Acta **1188:**1–28.
23. **Lewis, R. N., R. George, and R. N. McElhaney.** 1986. Structure-function investigations of the membrane (Na^+ + Mg^{2+})-ATPase from Acholeplasma laidlawii B: studies of reactive amino acid residues using group-specific reagents. Arch. Biochem. Biophys. **247:**201–210.
24. **Nguyen, T. X., M. R. Yen, R. D. Barabote, and M. H. Saier, Jr.** 2006. Topological predictions for integral membrane permeases of the phosphoenolpyruvate:sugar phosphotransferase system. J. Mol. Microbiol. Biotechnol. **11:**345–360.
25. **Pirch, T., S. Landmeier, and H. Jung.** 2003. Transmembrane domain II of the Na^+/proline transporter PutP of Escherichia coli forms part of a conformationally flexible, cytoplasmic exposed aqueous cavity within the membrane. J. Biol. Chem. **278:**42942–42949.
26. **Poelarends, G. J., and W. N. Konings.** 2002. The transmembrane domains of the ABC multidrug transporter LmrA form a cytoplasmic exposed, aqueous chamber within the membrane. J. Biol. Chem. **277:**42891–42898.
27. **Postma, P. W., J. W. Lengeler, and G. R. Jacobson.** 1993. Phosphoenolpyruvate:carbohydrate phosphotransferase systems of bacteria. Microbiol. Rev. **57:**543–594.
28. **Schnetz, K., S. L. Sutrina, M. H. Saier, and B. Rak.** 1990. Identification of catalytic residues in the β-glucoside permease of E. coli by site-directed mutagenesis and demonstration of interdomain cross-reactivity between the β-glucoside and glucose systems. J. Biol. Chem. **265:**13464–13471.
29. **Sun, J., and H. R. Kaback.** 1997. Proximity of periplasmic loops in the lactose permease of Escherichia coli determined by site-directed cross-linking. Biochemistry **36:**11959–11965.
30. **Sun, J., J. Voss, W. L. Hubbell, and H. R. Kaback.** 1999. Proximity between periplasmic loops in the lactose permease of Escherichia coli as determined by site-directed spin labeling. Biochemistry **38:**3100–3105.
31. **Tang, X. B., M. Kovacs, D. Sterling, and J. R. Casey.** 1999. Identification of residues lining the translocation pore of human AE1, plasma membrane anion exchange protein. J. Biol. Chem. **274:**3557–3564.
32. **van Montfort, B. A., G. K. Schuurman-Wolters, J. Wind, J. Broos, G. T. Robillard, and B. Poolman.** 2002. Mapping of the dimer interface of the Escherichia coli mannitol permease by cysteine cross-linking. J. Biol. Chem. **277:**14717–14723.
33. **Wang, T.-W., H. Zhu, X.-Y. Ma, T. Zhang, Y.-S. Ma, and D.-Z. Wei.** 2006. Mutant library construction in directed molecular evolution. Mol. Biotechnol. **34:**55–68.
34. **Yagur-Kroll, S., and O. Amster-Choder.** 2005. Dynamic membrane topology of the Escherichia coli beta-glucoside transporter BglF. J. Biol. Chem. **280:**19306–19318.
35. **Zhou, J., R. T. Fazzio, and D. F. Blair.** 1995. Membrane topology of the MotA protein of Escherichia coli. J. Mol. Biol. **251:**237–242.